

Surface Morphology and Optical Studies of Non-aqueous Bi₂S₃ Thin Films

R.S. Mane¹, J.D. Desai², Oh-Shim Joo² and Sung-Hwan Han^{1*}

¹Inorganic Nano-Materials Laboratory, Department of Chemistry, Hanyang University, Sungdong-Ku, Haengdang-dong 17, Seoul, Korea 133-791

²Eco-Nano Research center, Korea Institute of Science and Technology, P.O. Box 131, CheongRyang, Seoul, Korea.

*E-mail: shhan@hanyang.ac.kr

Received: 26 October 2006 / Accepted: 6 January 2007 / Published: 1 February 2007

A high purity, amorphous Bi₂S₃ thin film composed of loosely packed nanometer-sized spherical grains has been successfully deposited onto ITO substrate at room temperature from non-aqueous bismuth nitrate and sodium thiosulphate solution using a simple, inexpensive, reproducible, and environmentally friendly chemical route method. Film was characterized for structural, surface morphological, optical properties by means of X-ray diffraction (XRD), scanning electron microscopy (SEM) and UV-vis spectrometer, respectively. In last section, Bi₂S₃ film on ITO substrate was utilized in photo-electrochemical (PEC) solar cell as a working and platinum as a reference electrode in presence of 80 mW/cm² light intensity in lithium iodide as an electrolyte. Film of non-aqueous Bi₂S₃ exhibits two separate direct band transitions. Existence of two separate direct transitions was firstly noted in Bi₂S₃ thin films and explained its possible causes. PEC analysis confirms n-type conductivity.

Keywords: Chemically modified electrode; Glutamic acid; Hydroquinone; Catechol; Electrochemical determination

1. INTRODUCTION

Bismuth trisulphide (Bi₂S₃) V-VI class of materials find special applications in photo-electrochemical cells, solar absorber coatings, thin film lithography as its forbidden energy gap is 1.7 eV [1]. Chemical deposition of bismuth trisulphide thin films has been reported using different sulfur releasing sources such as sodium thiosulphate, thiourea, and thioacetamide [2-5] with different structural, optical and electrical properties. Use of aqueous nanocrystalline Bi₂S₃ thin films in photo-electrochemical cells and photo-electrochemical performance with grain sizes were reported in our

previous studies [6], however, the conversion efficiency was too low and attributed to high value of series resistance and interfacial states in the cell, which were responsible for recombination mechanism. Killedar et al [7] reported non-aqueous deposition of Bi_2S_3 thin films with polycrystalline crystal structure in non-aqueous medium using spray pyrolysis method. Use of spray pyrolysis was extended by Kebbab et al [8] for studying optical and photoconducting properties of Bi_2S_3 thin films. Inclusion of Bi_2S_3 nanoparticles in polypyrrole thin films electropolymerized on chemically deposited bismuth sulfide electrodes and its effect in the protection mechanism is recently studied by Rincon et al [9, 10]. In addition to photoperformance, hydrogen photoproduction from hydrogen sulfide on Bi_2S_3 catalyst was carried out by Bessekhoud et al [11].

In present work, structural, surface morphological and optical properties of Bi_2S_3 thin films prepared from non-aqueous bath on ITO substrate were carried out by using X-ray diffraction (XRD), scanning electron microscopy (SEM) and UV-visible photo-spectrometer techniques, respectively. In last phase, attempt was made to utilize non-aqueous Bi_2S_3 film in electrochemical cell as a working electrode, with platinum as a counter electrode and studied photo-electrochemical performance in dark and in 80 mW/cm^2 light intensity using 0.1 M lithium iodide as an electrolyte.

2. EXPERIMENTAL DETAILS

In the present investigation, all the starting precursors were general-purpose reagents, used as available commercially. Bismuth nitrate ($\text{Bi}(\text{NO}_3)_3 \cdot 5\text{H}_2\text{O}$) (Oriental Chemical Industries make- 99 %) was dissolved in acetic acid glacial (Kanto Chemical Co. Inc. make-36-38%) to prepare a 0.1 M solution. Sodium thiosulphate was dissolved in formaldehyde, since it is insoluble in acetic acid (with 2-3% H_2O and neglected due to low concentration). This gives a solution mixture of miscible solvents. Then equal volumes of 0.1 M solutions were mixed in a 250 ml beaker and stirred for a few minutes. The pH of the resulting solution was 1.4. The colorless solution was found to turn yellow-brown in about 5-10 min, indicates initiation of the chemical reaction. Extremely, indium doped tin oxide (ITO) were used as substrates and cleaned using standard procedure described elsewhere [12] and kept dipping vertically in the beaker containing the reacting solution. At room temperature (27°C), after about 3 h deposition time period thin homogeneous Bi_2S_3 films were obtained. The films were washed with distilled water and dried in air.

3. CHARACTERIZATION

For the structural, surface morphological, optical, and photo-electrochemical characterizations of Bi_2S_3 non-aqueous thin film, ellipsometer, X-ray diffraction (XRD), scanning electron microscopy (SEM), UV-vis spectrophotometer techniques were used. During X-ray scanning, $\text{Cu-K}\alpha$ radiation of wavelength 1.5428 \AA used. High intensity $\text{Cu-K}\alpha$ X-rays obtained, after passing through $k\beta$ filter and a counter monochromator, were employed for diffraction experiments. Beam divergence was always restricted with the help of a 0.15 mm slit on the source side. The drive axis was 2θ for a scan range of $10\text{-}80^\circ$ with step size of 0.05° . Surface morphology study was carried out by SEM analyses with unit

Cambridge Stereoscan 250-MK. Optical absorption study was carried out in the wavelength range 350-850 nm. While measurement, standardization was done with reference ITO substrate (zero adjustment) with same thickness and sheet resistance $19 \Omega /\text{cm}^2$. I-V characteristic of photo-electrochemical cell with Bi_2S_3 as a working electrode was performed by using xenon flash lamp (450 W, Thermo Oriel Co. USA) under $80 \text{ mW}/\text{cm}^2$ illumination intensity.

4. RESULTS AND DISCUSSION

4.1 Film formation mechanism

Bi_2S_3 thin film formation takes place in non-aqueous medium. Here, reaction takes place between the dissolve precursors in the solution. When the solution is saturated ionic product is equal to solubility product and when it exceeds, precipitation occurs and ions combine on the substrate and in the solution to form nuclei. The required number of ions has sufficient space and time to combine on the substrate and in the solution to form nuclei, which grow slowly by the combination of more ions to develop the film on the substrate (ITO) and in the solution to form precipitate, respectively. Ion-by-ion deposition takes place depending upon the preparative conditions such as bath temperature, pH, solution concentration etc. Solubility product of metal chalcogenide depends on temperature, control over ion concentration and hence growth rate is feasible by controlling the temperature of the deposition bath. Due to low temperature process we believe lower the kinetic energy of ions and controlled dissociation. At some in-homogeneities formation of nucleation generally prefers. Slow release of metal ions with decrease in reaction bath temperature results into formation of fine metal chalcogenide thin films [13]. In previous reports [14-15] mechanism of Bi_2S_3 film formation was reported in detail using the concept of solubility product (actual values). Measurement of film thickness by ellipsometer was $455 \pm 2 \text{ nm}$ at different positions of film.

4.2 Structural studies and surface morphology

Crystallinity of Bi_2S_3 film was examined by X-ray diffraction, where, low intensity Bi_2S_3 peaks reveals low crystallinity and/or amorphous structure of the film. Very few peaks of relatively low intensity were detected and showed good matching with the JCPDF card 17-0320. Due to amorphous nature and large background peaks we were incapable to measure grain size. Observed two weak peaks are mostly appeared in the background noise, so to confirm Bi_2S_3 structure we carried out energy dispersive X-ray spectroscopy (EDX) (not shown) that was well supporting for the formation of Bi_2S_3 films with 2:3 composition. Such films may be useful as (buffer) layers for certain devices, but if deposited at room temperature, good crystallinity is not expected [16], and indeed not obtained here (Fig.1 almost only substrate peaks). Fig.2 shows SEM image of Bi_2S_3 thin film deposited from aqueous bath at 10,000 x magnification. The surface morphology is found to be little different than the earlier reports, where exact and crowded spherical smooth grains Bi_2S_3 were detected. However, little rough spherical boundaries of grains are clearly seen in SEM image. All grains are found to be of same nature with little grain size difference ($\pm 10 \text{ nm}$). Due to compact, sufficiently large grain size and

uniform distribution over the given substrate surface area of less magnification image, here we measured grain size by using well known bar code system; drawing cross bars of same dimensions as provided scale and measuring number of intersecting grains across them. The average grain size was 224 ± 10 nm.

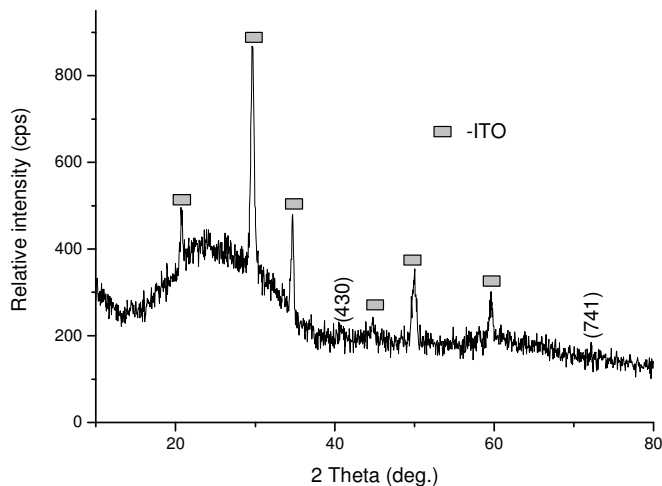


Figure 1. XRD pattern of Bi_2S_3 thin film synthesized from non-aqueous bath on ITO coated glass substrate.

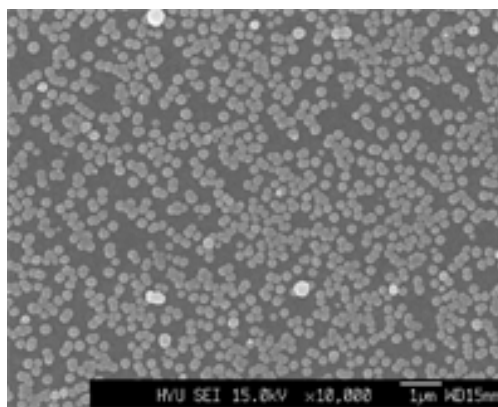


Figure 2. SEM image of Bi_2S_3 film synthesized from non-aqueous medium under magnifications 10 K.

4.3 Optical studies

Fig. 3 (a, b) shows the optical absorption spectrum recorded at room temperature with wavelength of incident photon. Using other ITO as a reference compensates with the contribution of ITO substrate to band gap of Bi_2S_3 . Careful observation in absorption spectrum leads to conclude presence of two absorption edges, one at high wavelength (696 nm) and other at low wavelength (375 nm), respectively. Both edges are complicated and supposed to be strongly depends on incident photon energy, indicating presence of more than one transition. Due to high absorption coefficient the data

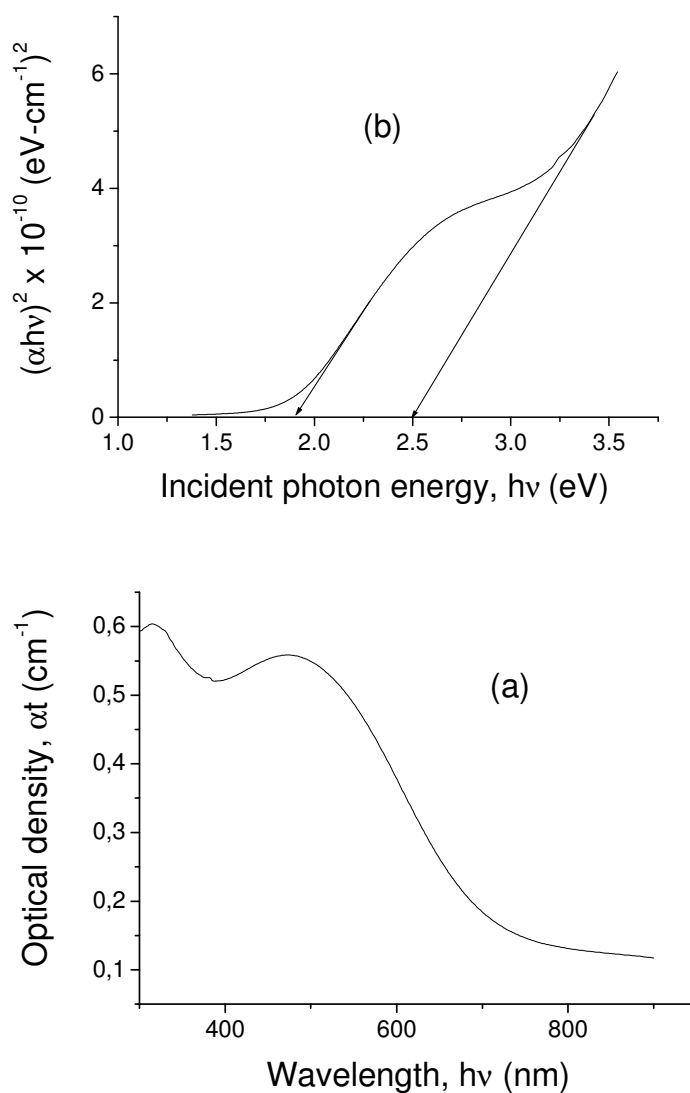


Figure 3. (a) A plot of observed absorbance (optical density) dependence of wavelength of incident photons. Two distinct transitions at 375 and 696 nm are clearly distinguished and (b) variation of $(\alpha h\nu)^2$ versus $h\nu$ whose extrapolation to zero absorption gives direct band gaps

was analyzed in the vicinity of absorption edge by computing the values of absorption coefficient at every 1 nm wavelength. These observed experimental results could be interpreted with the help of equations derived from the single crystal where incident photon energy must be greater than the band gap energy [17,18] as $\alpha = A (h\nu - E_g)^n / h\nu$, where $h\nu$ is the incident photon energy, and A , n are the constants. n must possess the values $1/2$ and 2 for allowed direct and indirect transitions, respectively. It is possible to determine nature of transitions involved, by plotting the graphs of $(\alpha h\nu)^n$ versus $h\nu$ for different values of 'n' as described above. One can obtain the energy gap (band gap energy) by

extrapolating the straight-line portion of graph to zero absorption coefficient. The plot shows a linear dependence at photon energy greater than band gap energy, therefore extrapolation of straight line portions of the curve to zero absorption gives band gaps at $E_{g1} = 1.90$ and $E_{g2} = 2.5$ eV, respectively. This may be the first report of existence of two-band gap energies in Bi_2S_3 thin films from non-aqueous medium. But theoretical study do not predicts the existence of second band transition of the Bi_2S_3 films. The lower energy optical transition at 1.90 eV is due to the allowed direct transition from the top of valence band to the conduction band minimum at the center of the Brillouin zone and was found to be very close to reported values for Bi_2S_3 thin films [7]. However this study reveals the dielectric function of Bi_2S_3 reveals a spin-orbit split of 0.8 eV for the fundamental 1.7 eV. This value is larger than the standard which mainly attributed to extremely thin films and nanocrystalline/amorphous, compact grain structure. We can infer that the band gap energies are partially dependent on the crystallinity of the thin films. As the band gap energies for well-crystallized thin films are comparable with those of crystallized bulk materials, whereas for the amorphous or poorly crystallized once, the band gap energies are higher than those of the corresponding bulk materials, which is also supported by other studies [19, 20]. Observed higher energy transition at 2.5 eV is may be due to the transition from the spin-orbit split valence band to the conduction band. In literature, 2.1 eV band gap direct band gap energy of Bi_2S_3 thin films is reported by Al-Douri and Madik [21]. Here, for second transition in film, artifact related to the morphology of the film, bulk inhomogeneities like voids (air inclusions) and roughness surface [22] may be other unknown responsible contributing parameters.

4.4. Photo-electrochemical studies

Photo-electrochemical cell of was designed using Bi_2S_3 as a working electrode, platinum as a counter electrode and 0.1 M lithium iodide as an electrolyte under the light illumination of intensity 80 mW/cm^2 .

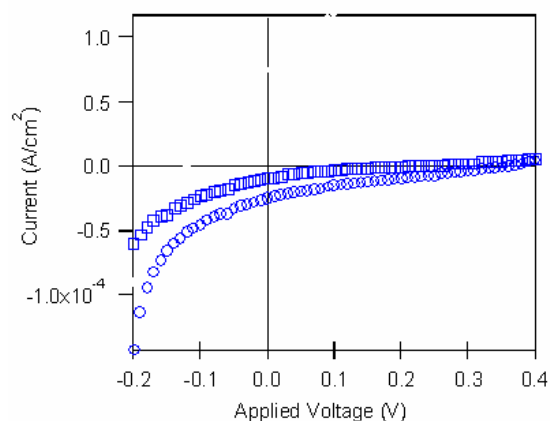


Figure 4. *I-V* characteristics of Bi_2S_3 thin film as a working electrode and platinum as a counter electrode. Square and circle represents dark and light performance of cell in lithium iodide as an electrolyte.

The cell was made using cello tape and electrolyte was introduced into it more carefully using non-toxic 1 mL syringe. Film shows some dark current and voltage, respectively and attributed to difference between two half-cell potentials in PEC cells ($E = E_{\text{platinum}} - E_{\text{Bi}_2\text{S}_3}$), where platinum was at positive polarity and working electrode at negative polarity ends, respectively. Here, E_{platinum} and $E_{\text{Bi}_2\text{S}_3}$ are the half-cell developed potentials when comes in contact of lithium iodide electrolyte. After light illumination, the magnitude of voltage increases with negative polarity towards Bi_2S_3 thin film and cathodic behavior was detected confirmed n-type conductivity. n-type conductivity of Bi_2S_3 is well known. Fig. 4 shows the dark and light I-V characteristics of Bi_2S_3 thin film. Increase in current with well rectification in fourth quadrant supports previous analysis. Device conversion efficiency was small (0.002%). Considerable change in open circuit voltage was recorded (0.19 to 0.35 V) however short circuit current was low (0.009 and 0.024 mA/cm²). In overall, this is due to low fill factor i.e. 0.21%, which leads to form low conversion efficiency. Poor fill factor is attributed to many reasons such as large spacing between the grains and rough grain boundary surfaces, which lead to increase series resistance of the cell resulting [23, 24].

5. CONCLUSIONS

An environmentally friendly non-aqueous system for fabricating Bi_2S_3 thin film on ITO substrate at room temperature has been successfully developed. Films were used for their structural and surface morphological characteristics showing amorphous structure with spherical grains having rough surfaces and void space. This result restricts us to use film in photo-electrochemical cells but can be used in devices as a buffer layer. Two direct transitions were detected, out of which lower 1.91 eV was related to top of valence band and bottom of conduction band and higher 2.5 eV may be due to transition from the spin-orbit split valence band to the conduction band. I-V characteristics confirmed n-type behavior of the Bi_2S_3 with enhancement in power conversion efficiency under the light intensity 80 mW/cm².

ACKNOWLEDGEMENTS

This work was supported by the Korean Science and Engineering Foundation (ABRL R14-2003-014-01001-0). One of the authors, RSM wishes to thank Korean federation of Science and Technology Societies (KOSEF), Korea for the award of Brain pool fellowship (2006-2007).

References

1. R.S. Mane, B.R. Sankapal, C.D. Lokhande, *Thin Solid Films* 359 (2000) 136.
2. J.D. Desai, C.D. Lokhande, *Mater. Chem. Phys.* 41 (1995) 98.
3. J.D. Desai, C.D. Lokhande, *Mater. Chem. Phys.* 34 (1993) 313.
4. R.S. Mane, B.R. Sankapal, C.D. Lokhande, *Mater. Res. Bull.* 35 (2000) 587.
5. C.D. Lokhande, B.R. Sankapal, R.S. Mane, H.M. Pathan, M. Mullere, H. Tributsch, V. Ganeshan, *Appl. Surf. Sci.* 187 (2002) 108.
6. R.S. Mane, B.R. Sankapal, C.D. Lokhande, *Mater. Chem. Phys.* 60 (1999) 158.
7. V.V. Killedar, C.D. Lokhande, C.H. Bhosale, *Thin Solid Films* 289 (1999) 14.

8. Z. Kebbab, N. Benramdane, M. Medles, A. Bouzidi and H. Tabet-Derraz, *Solar Energy Mater. Solar Cells*, 71 (2002) 449.
9. M. E. Rincón, H. Hu, G. Martínez, *Synthetic Metals*, 139 (2003) 63.
10. M. E. Rincón, H. Hu, G. Martínez, R. Suárez and J. G. Bañuelos, *Thin Solid Films*, 431 (2003) 131.
11. Y. Bessekhoud, M. Mohammedi and M. Trari, *Solar Energy Mater. Solar Cells*, 73 (2002) 339.
12. C.D. Lokhande, E.-H. Lee, K.-D. Jung, O.-H. Joo, *J. Mater. Sci.* 39 (2004) 2915.
13. R.S. Mane, C.D. Lokhande, *Mater Chem. Phys.* 64 (2000) 215.
14. J.D. Desai, C.D. Lokhande, *Ind. J. Pure Appl. Phys.* 32 (1994) 964.
15. J.D. Desai, C.D. Lokhande, *Mater. Chem. Phys.* 41 (1995) 98.
16. R.S. Mane, C.D. Lokhande, *Thin Solid Films* 304 (1997) 56.
17. P.P. Hankare, V.M. Bhuse, G.M. Gardkar, S.D. Delekar, I.S. Mulla, *Semicond. Sci. Technol.* 19 (2004) 70.
18. R.B. Kale, S.D. Sartale, B.K. Chougule, C.D. Lokhande, *Semicond. Sci. Technol.* 19 (2004) 1.
19. Y. Gao, Y. Masuda, Z. Peng, T. Yonezawa, K. Koumoto, *J. Mater. Chem.* 13 (2003) 608.
20. D.G. Syarif, A. Miyashita, T. Yamaki, T. Sumita, Y. Choi, H. Itoh, *Appl. Surf. Sci.* 193 (2002) 287.
21. Ala A. J. Al-Douri and Maria P. Madik, *Ren. Energy*, 21(2000) 411.
22. N. Guezmir, J. Ouerfelli, S. belgacem, *Mater. Chem. Phys.*, (2005) in press.
23. R.S. Mane, C.D. Lokhande, *Mater. Chem. Phys.* 78 (2002) 383.
24. P.K. Nair, M.T.S. Nair, V.M. Garcia, O.L. Arenas, Y. Pena, A. Castillo, I.T. Ayala, O. Gomezdaza, A. Sanchez, J. Campos, H. Hu, R. Suarez, M.E. Rincon, *Solar Energy Mater. Solar Cells*, 52(1998)313.